MICRO-MECHANICAL MODELLING OF ASR

Cyrille Dunant, Amor Guidoum, Karen Scrivener

Laboratoire de Materiaux de Construction. Institut des Materiaux, EPFL.
EPFL-IMX-LMC Station 12, 1015 LAUSANNE, Suisse.

Abstract

In this paper, a method is described to model the effect of ASR at a microstructural level, using a modular finite element approach. Using back scattered electron microscopy on polished sections, it was found that ASR-induced cracks originate from reactive zones in the aggregate, and propagate into the cement matrix. Our approach uses both classical Lagrangian elements and extended finite elements (XFEM), to allow for dynamic changes in the sample geometry. The reaction is modelled as expansive zones within the aggregates and is coupled with a damage parameter for the initiation of cracks, which are then propagated using an energetic criterion. We have developed an automatic mesher which notably allows the generation of statistically significant numbers of numerical samples. The samples are created based on a set of macroscopic parameters such as porosity and aggregate size distribution, and the effect of variability is evaluated. We demonstrate how the model can explore the relationships observed experimentally between chemical reactivity and microscopic expansion.

Keywords: ASR, Finite Element, Modelling, XFEM, Prognosis.

1 INTRODUCTION

ASR is an important durability concern for mass concrete structures. It affects both their structural integrity and their functionality. In most studies, the effect of the reaction is generally modelled at the structural level, with behaviour laws and boundary conditions designed to emulate the expansion as a function of external parameters such as temperature and hygrometry [1]. At the other end of the spectrum, the effect of ASR can be understood at the level of the concrete mesostructure, using either direct methods for the simulation of single aggregates [2], or analytical models such as those of Bažant and colleagues coupled with homogeneisation techniques [3]. Simulation of fracture mechanics at the meso-scale has already been attempted by Schlangen and Garbozi using a lattice model on small-scale surfaces [4], or at a larger scale by Van Mier and Van Vliet [5].

This paper presents the implementation of numerical methods which allow simulations of numerical samples of sizes comparable to that commonly used in laboratory experiments at the level of the microstructure. To this end we have developed a simulation framework capable of handling the large number of degrees of freedom this problem entails, and mesh-free (mesh independent) methods capable of capturing the physics of the phenomenon. The model presented here is in two dimensions but can be extended to three-dimensional simulations using the same simulation framework we have developed. Fracture initiation and propagation uses a non-local kill-element scheme, with an energy-based criterion.

2 EXPERIMENTAL OBSERVATIONS

Ben Haha [6] carried out expansions tests with concretes and mortars cast with moderately reactive aggregates at different temperature and alkali levels. This experimental study is being continuing with different aggregates.

Aggregates used in dam constructions were first evaluated for their reactive potential using the AFNOR norm "microbar" test [7], and were classified according to the norm as potentially reactive. The Microbar protocol measures the expansion of small (4 ×1 × 1 cm) mortar bars after 6 hours immersed in a 2.4 molar NaOH solution at 127 °C.

Mortar and concrete samples were prepared with the aggregates and cured under various temperature conditions. Polished sections were prepared for BSE observations at regular time intervals.

These experiments provided both qualitative and quantitative data which highlight some properties of the effects of ASR at the micromechanical level: heterogeneous reactivity of the aggregates, relation between the reacted fraction of the aggregates and the observed macroscopic expansion, cracking patterns.

2.1 Gel localisation

The aggregates evaluated using the procedure described in the AFNOR norm [7] for mortar bar test. At various time points the samples which were cast according to the norm were sawed, impregnated in epoxy and polished for observation under the electron microscope (Figure 1).
The reacted zones were found to be distributed throughout the aggregates. Similar observations were made on both concrete and mortar samples [6].

Most of the analysis was performed by Ben Haha [8]. Three mineralogically different aggregates where used in the mortars and concretes, which cured at three different temperatures (20, 40 and 60 °C) with varying alkalinity levels in the cement.

The expansion was measured until the samples had stopped expanding. The varying cure condition gave insights on how the cure parameters affect the kinetics of expansion. The following relation was established with respect to temperature and alkali concentration:

$$expRate = [a]^g e^{\frac{T}{E_a}} f[t]$$

Where expRate is the rate of expansion, [a] is the alkali concentration, g a factor, T the temperature, E_a the apparent activation energy (43.5 ± 2 Kj·mol^{-1} from Ben Haha [8]) and f(t) some function of time and other parameters affecting the kinetic of the reaction.

Ben Haha found a unique relation between expansion and reacted fraction. A renormalisation function taking into account the aggregate fraction was found which allowed the comparison across samples with varying grain size distributions (Figure 2).

3 MODELLING

The experimental observations were used as a guide to the development of our simulation framework, which was engineered to enable us to reproduce numerically the experimental data using finite element modelling (FEM).

3.1 Numerical setup

Based on the experimental evidence, a two-dimensional micro structural model of ASR affected concrete was put together. The basis of the simulation is 16 × 4 mm mortar bars using a model that is statistically geometrically accurate and micro mechanically simple.

The aggregates and reactive zones are represented individually, which lead to a complex geometry. Despite this, the mechanical behaviour of the various features used in the model setup are simple: linear elasticity, prescribed strains for the ASR gel, and a Mohr-Coulomb criterion for fracture propagation and initiation. The two-dimensional approach, assuming plane stress, is a first approach to represent the three-dimensional nature of the problem, but the computational framework allows for extension to 3 dimensions at a later stage.

The Geometry is represented using a conformant meshing for the fixed part, aggregates and paste, and XFEM for the expansive zones for which the geometry varies with the simulation steps. This combination allies flexibility and numerical efficacy.

Aggregates and paste

We model our aggregates using a circular geometry as this helps us to generate grain size distributions similar to that of the experimental samples. The aggregates have a fixed geometry throughout the expansion history of the sample. For the sake of numerical efficiency, the aggregates were meshed using a conformant mesh. To that effect, a Delaunay mesher was implemented with an algorithm adapted from Devillers and colleagues [9], specially tailored for unsupervised tessellation.

The geometrical setup reproduces the grain size distribution (GSD) of the aggregates in real mortar samples, at least 99% of the total aggregate mass is accounted for with an aggregate content of the sample above 60%. The ratio between the largest and the smallest aggregate is ≈ 22. For a mortar, this means that the smallest aggregate represented has a diameter of 0.089 mm. Small aggregate size fractions are believed to behave like pozzolans and not participate significantly to the reaction. Poyet [11] shows that even for fully reactive aggregates (recycled glass) small grain sizes (median size of 0.175 mm) yield small expansions. Thus the aggregate density obtained is sufficient for the simulation.

Fracture simulation is done using a non-local kill-element scheme using an energetic criterion for fracture propagation. Cracks are initiated at the points where in a given region of the mesh the maximum principal stress is reached, and the mechanical simulation loops until cracks have stopped propagating (no more elements reach the fracture criterion). To better represent the heterogeneity of

the material, as well as stabilise the crack propagation, the mechanical properties of the elements are randomised using a Weibull distribution.

Reactive zones

Reactive zones are not modelled using a conformant mesh. Instead, they are represented using soft discontinuities introduced with XFEMs. Reactive zones are distributed randomly inside the aggregates. The number of reactive zones per aggregate is proportional to its area. the size of these reacted zones is independent of the aggregate size. This is based on the assumption that morphology of the reactive material is constant in the material. Thus a small aggregate might be fully reactive or not at all, whereas larger ones will probably always be partly reactive.

The fraction of the aggregates which has reacted at various time points is derived from the experimental data. The steps of the simulation have to be sufficiently small that quasi-static conditions can be assumed: the cracks grow slowly with the expansion of the reacted zones and are not the result of a shock induced by the rapid reaction of a large fraction of the aggregate.

Experimentally it was found that the expansion is related to the fraction of the aggregates which has reacted, independent of time, and as the behaviours used in the simulation are all linear, the radius of the reactive zones varies linearly so that the reacted area goes from zero to three percent of the aggregates area during the simulation.

Remeshing such fine features as reactive zones at each step would be time consuming, as well as induce the risk of forming badly conditioned matrices. Simulating the reactive zones with extended finite elements such as those introduced by Babuska and co-workers [12] makes the remeshing step optional. To capture the effect of the interface between the gel and the aggregate, a C^1 discontinuous hat function was used as enrichment. Using an enrichment scheme has the additional interest that it allows elements to conserve their history throughout the simulation.

At each step of the simulation, the geometry of the gel zones is updated. The elements fully contained in the reacted zones are attributed an expansive behaviour, the elements containing a gel-aggregate interfaced are enriched with the supplementary shape functions and a bi-material behaviour is attributed (Figure 3).

This step is computationally very costly due to the considerable amount of reactive zones to treat (up to 20 000 in detailed samples). Our mesher is designed to provide fast searching capabilities to optimise this step of the computation [13](Figure 4).

Mechanical modelling

The mechanical behaviour of the components is simple linear elastic. The expansive zones have an imposed strain. The mechanical properties of the paste and the aggregates are known, from experiments and literature. Thus the only unknown is the behaviour of the gel.

The properties of ASR gel reported in the literature [14] vary widely and furthermore the properties of the gel when it causes expansion are not necessarily the same as when it is examined later. The chemical composition of the gel varies depending on the calcium content, from a quasi-liquid sodium-silicium gel, which can be assumed to have the mechanical properties of water, to the composition of C-S-H [18]. However, the effect of the gel can be inferred from the overall expansion behaviour. We have elected to make the gel quasi-incompressible (Poisson ration = 0.49999) and the model is refined for two parameters:

- the ratio of total gel volume to total aggregate volume.
- the Young's modulus of the gel.

This seemingly simple assumption is justified by the fact that the expansion-reaction curve seems to be independent of aggregates and curing conditions. This implies that even if the mechanical properties of the gel are not linear elastic, this assumption is sufficient to well reproduce its effect on the aggregate.

The refinement is performed on only the Young's modulus, as the variation of either the expansive ratio or the stiffness have the same effect on the applied stress.

4 OBSERVATIONS

4.1 Numerical simulations

Model stability

The number of modelling steps was adjusted to capture the dynamic of the model. This is important because reducing the number of simulation steps is desirable, if no information is lost. As cracks are simulated using a damage model at present, it becomes impossible to continue the simulation beyond the point at which parts of the sample detach.

This point coincides with the experimental strain limit of concrete (≈ 0.02%) At this point, the cement matrix cracks and large parts of the simulated sample become detached. The presence of solid body modes in the finite element solution prevents convergence as no unique solution exists at that point.

Cracking patterns

While large expansions lead to macroscopic cracking [15], even small expansions lead to micro cracks observable under the SEM as illustrated in Figure 5. Star-like crack patterns originating from reactive zones are observed.

For the aggregates observed in this study, cracks were first observed in the aggregates, between the pockets of gel, then, as the reaction develops, they grow through the aggregates, and then penetrate the matrix. To get the original state of the aggregate, samples were prepared for observation immediately after demolding.

The differential expansion induced by the aggregates in the specimen and the non-expanding paste induces cracking where the tensile stress is maximum. This is on the surface of the specimen, where only paste is present and no external stress is present to keep the paste under compression. In the two dimensional simulation this leads to cracks initiating at regular intervals from the surface, which may partly explain the map-cracks which are typically observed on ASR affected structures. Figure 6 illustrates such a pattern.

Effect of the gel mechanical properties

We have run a series of numerical experiments varying only the Young's modulus of the gel (Figure 7). These experiments indicate that the expanding gel can be considered as a boundary condition, which does not affect the apparent behaviour of the simulated sample. Thus, given the reacted fraction, the effect of varying the modulus of the gel is simply a scaling effect on expansion.

Due to the highly concentrated nature of the induced stresses, the cracks initiate at the same point of expansion, and their propagation is not significantly different, if the induced stress is sufficient to initiate the crack propagation. However, the total expansive load applied on the structure varies with the gel stiffness. This explains why the shape of the curves remains similar, while the scale changes.

5 DISCUSSION

The simulated expansion curves tend to indicate that the effect of the gel on the microstructure can be considered as a boundary condition that depends very little on the real behaviour of the ASR gel, which is very difficult to determine experimentally. To study this finding, further simulations will look at the effect of ASR on the mechanical properties of the material. The numerical model leads to the interpretation of the expansion reaction curve illustrated in Figure 8. After an initial linear expansion the aggregates start cracking due to gel pressure. The gel then builds up pressure in the cracked aggregate, and cracks initiate and propagate in the paste.

This model can be used to generate a material-level homogenised damage model, linking the advancement of the reaction with the deterioration of the material.

Knowing the reactive fraction and localisation of the reactive zones within the aggregates suffices to be able to simulate the expansion of ASR-affected concrete. If the geometry of the problem is sufficiently well represented, simple behaviour laws capture the essence of the mechanical response of the microstructure.

6 CONCLUSION

This paper shows that it is possible to make a micromechanical simulation reproducing the observed reaction-expansion behaviour of ASR-affected concrete. We find that the non-local kill-element scheme used was sufficient to simulate qualitatively the cracking pattern observed in real samples. However it was also found to be limited when the strain limit of the cement matrix is reached by the simulated sample, which limits the quantitative output the model can produce in its current stage. At this point of the simulation convergence become hard to obtain, and computed strains cease to be meaningful.

The kinetics of the reaction could be reproduced by matching amounts of gel produced with time. This would allow to couple the simulation with time-dependant behaviours such as creep.
Further development will concern the use of XFEM also for the simulation of cracks, for better treatment of fracture behaviour.

7 REFERENCES

[1] Fairbairn, E. M. R., Ribeiro, F. L. B., Lopes, L. E., Toledo-filho, R. D., and Silvoso, M. M. (2005). Modelling the structural behaviour of a dam affected by alkali–silica reaction. Commun. Numer. Meth. Engng, (22):1–12.

[2] Çopuroglu, O. and Schlangen, E. (2007). Modelling of effect of ASR on concrete microstructure. Key Engineering Materials, 348:809–812.

[3] Bažant, Z. P. and Steffens, A. (1999). Mathematical model for kinetics of alkali-silika reaction in concrete. Cement and Concrete Research, (30):419–428.

[4] Schlangen E. and Garboczi E. J. (1997) Fracture Simulation of Concrete using Lattice Models: Computational aspects. Engineering Fracture Mechanics, (57):319-332

[5] Van Mier J. G. M. and Van Vliet M. R. A. (2003) Influence of microstructure of concrete on size/scale effects in tensile fracture. Engineering Fracture Mechanics, (70):2281-2306.

[6] Ben Haha, M. (2006). Mechanical Effects of Alkali Silica Reaction in concrete studied by SEM image analysis. PhD thesis, EPFL.

[7] AFNOR (2004). Methodes d'essai de reactivite aux alcalis.

[8] Ben Haha, M., Gallucci, E., Guidoum, A., and Scrivener, K. L. (2007). Relation of expansion due to alkali silica reaction to the degree of reaction measured by sem image analysis. Cement and Concrete Research, 37(8):1206–1214.

[9] Devillers, O., Meiser, S., and Teillaud, M. (1992). Fully dynamic Delaunay triangulation in logarithmic expected time per operation. Comput. Geom. Theory Appl., 2(2):55–80.

[10] Mehta, P. K. and Monteiro, P. J. (2006). Concrete: microstructure, properties and materials. McGraw-Hill.

[11] Poyet, S. (2003). Etude de la degradation des ouvrages en beton atteints par la reaction alcali-silice : Approche experimentale et modelisation numerique multi-echelles des degradations dans un environnement hydro-chemo-mecanique variable. PhD thesis, Universite de Marne-La-Vallee.

[12] Babuska, I. and Melenk, I. (1997). Partition of unity method. International Journal for Numerical Methods in Engineering, 40(4):727–758.

[13] Dunant, C., Vinh, P. N., Belgasmia, M., Bordas, S., and Guidoum, A. (2007). Architecture tradeoffs of integrating a mesh generator to partition of unity enriched object-oriented finite element software. Revue europeenne de mecanique numerique, 16:237–258.

[14] Perruchot, A., Massard, P., and Lombardi, J. (2003). Composition et volume molaire apparent des gels ca–si, une approche experimentale. C. R. Geoscience, (335):951–958.

[15] Amde, A., Ceary, M., and Livingston, R. (2005). Correlation between map cracking and delayed ettringite formation in field specimens. Number 11. 11th International conference on concrete.

[16] Bolomey, J. (1935). Granulation et prevision de la resistance probable des betons. Travaux, 30(19):228–232.

[17] Binal A. (2007), The determination of gel swelling pressure of reactive aggregates by ASGPM device and a new reactive-innocuous aggregate decision chart, Constr Build Mater doi:10.1016/j.conbuildmat.2007.07.021.

[18] Kawamura M. and Kazuma I. (2004) ASR gel composition and expansive pressure in mortars under restraint. Cement & Concrete Composites (26):47–56.

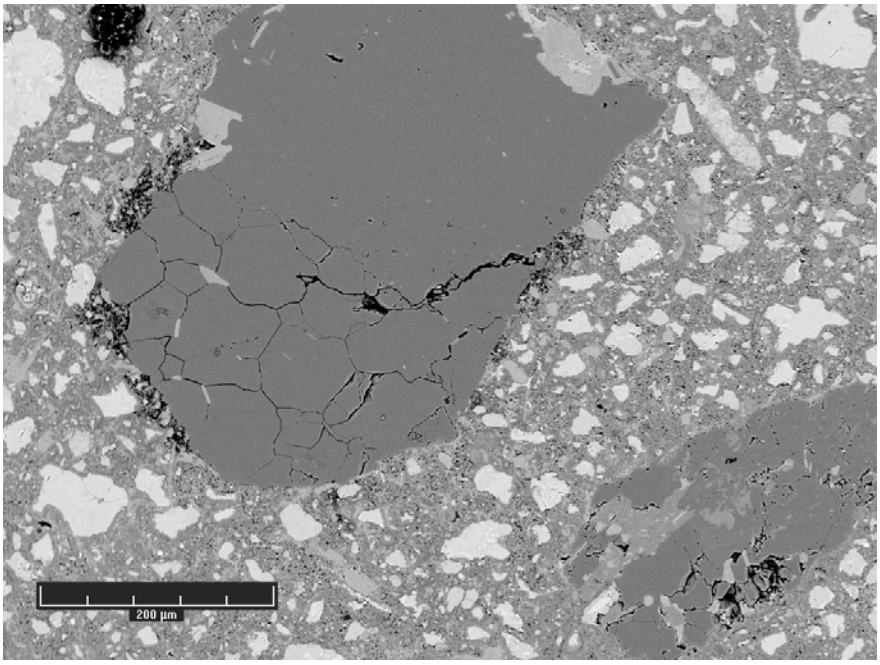

Figure 1: Micrograph of a sample after a MICROBAR test. One can clearly see the cracks initiating at the zones within the aggregates which reacted.

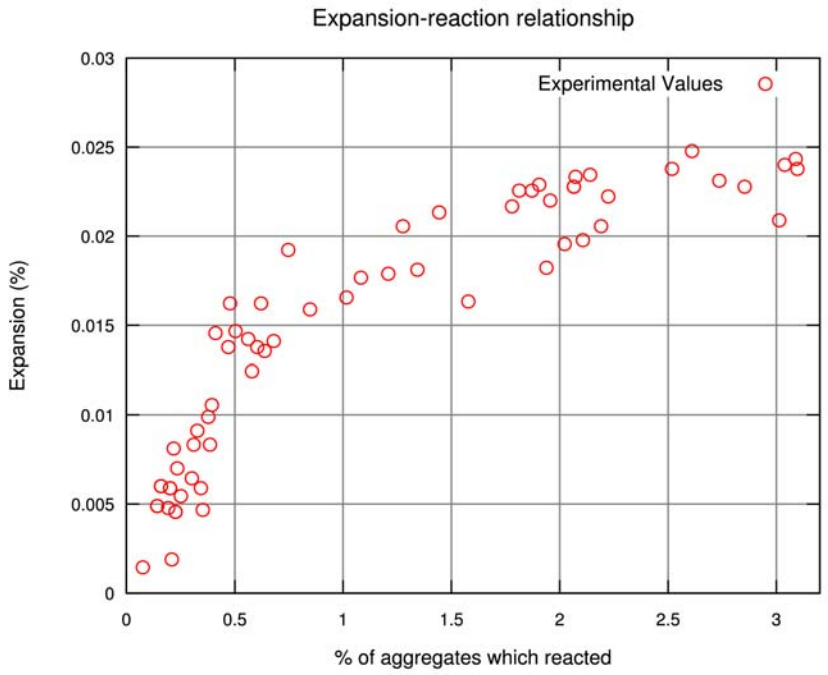

Figure 2: Experimental relationship between measured free expansion and measured reacted fraction. Both mortar and concrete expansions values are reported in this graph, after renormalisation of the concrete expansion values with respect to the relative aggregate content. Adapted from Ben Haha[8].

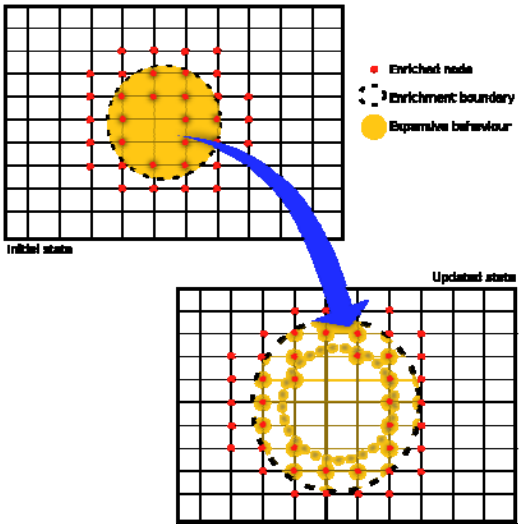

Figure 3: Update of the enrichment scheme. Enrichment nodes are updated according to the new geometry. Expansive behaviour is attributed to the elements and part-elements within the reacted zones. The enrichment strategy is independant of the mesh and mesh type: here a quadragular regular mesh is shown for clarity.

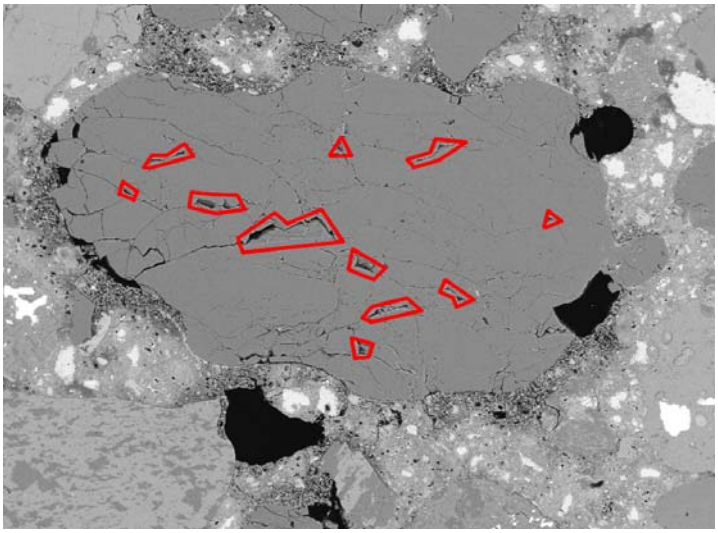

Figure 4: Star-like patterns originating from reactive zones are observed. Reactive zones are marked in red.

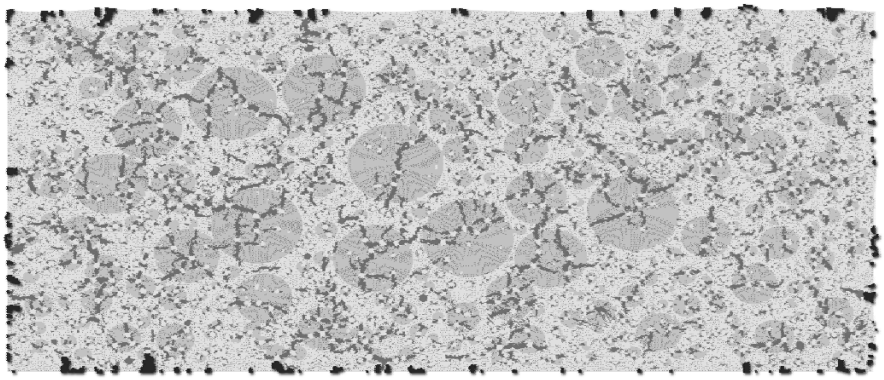

Figure 5: Map-cracks are highlighted in the simulation. In two dimensions, they are cracks initiating from the surface of the sample at regular intervals. This example is the result of a non-realistic simulation performed to highlight the mechanical consequences of the gel expansion.

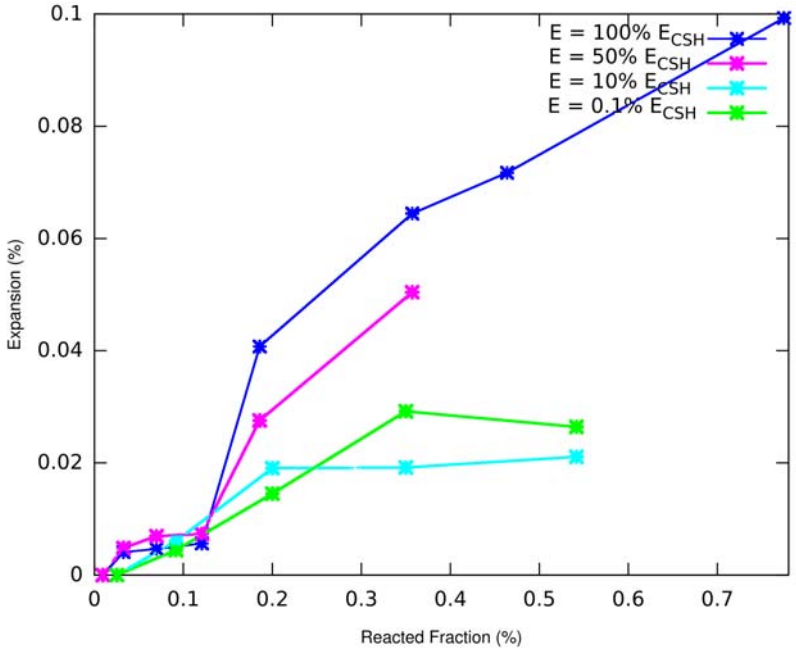

Figure 6: Simulated expansion-reaction curves. The parameter varied is the stiffness of the gel, all other parameters are kept constant. We see that simply varying this parameter does not affect the shape of the curve, but only scales it.

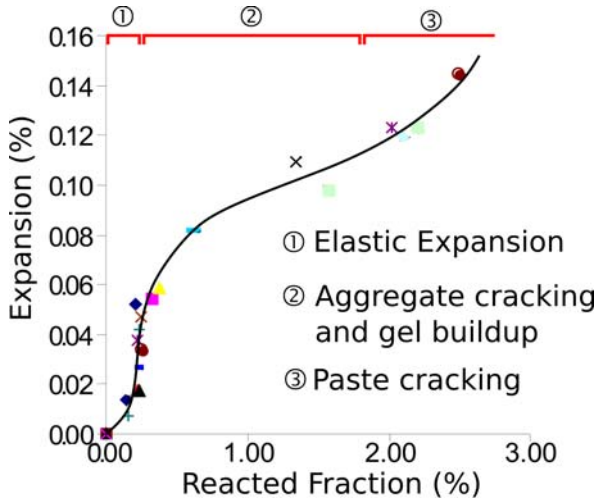

Figure 7: Experimental expansion-reaction curve (adapted from Ben Haha [8]). The phases in the ASR damage mechanism are highlighted.